Design of a Highly Sensitive Wireless Passive RF Strain Transducer

Trang T. Thai[1,2], Herve Aubert[1,3], Patrick Pons[1,3], Manos M. Tentzeris[2], and Robert Plana[1,3]

[1] CNRS ; LAAS ; 7 avenue du colonel Roche, F-31077 Toulouse Cedex 4, France
[2] School of ECE, Georgia Institute of Technology, Atlanta, GA 30332, U.S.A.
[3] Université de Toulouse ; UPS, INSA, INP, ISAE ; UT1, UTM, LAAS ; F-31077 Toulouse Cedex 4, France

***Abstract* — A highly sensitive wireless passive radio frequency strain transducer is designed and developed based on a patch antenna loaded with an open loop. A novel idea of utilizing a cantilever at the gap of the open loop significantly improves the sensitivity of resonant frequency shifts. The ground plane allows the sensitivity of the sensor to be independent from the applied surface. A proof-of-concept prototype is fabricated and the measurements successfully validate the operation principle.**

***Index Terms* — strain stress sensor, RF transducer, wireless passive sensing.**

I. Introduction

Strain is a critical parameter in structural health monitoring essential to many industries ranging from civil infrastructure, mechanical equipments, to aerospace as well as various medical applications. In civil structures, strain sensing is needed for safety assurance of roads, bridges, and building supports to avoid unexpected collapses [1]. In manufacturing processes and constructions, strain sensing allows the monitoring of vibration, excessive loading, and crack developments to be detected early [2]. Strain sensing in medical uses also include implantable sensors for bone, joint healing processes, and bone fracture monitoring [3]. In aerospace, strain is especially a sensitive parameter for operations of aircrafts, including the conditions of wings and blades, as well as fatigue of the aircraft body [4]. Strain is a parameter indicating a physical deformation and mechanical loading. Strain sensors have been widely developed utilizing different techniques [5], among which the most common types are resistive and capacitive gages which typically require wiring, and/or complex circuits adding weight penalty [6] that are especially highly undesirable for implementation on aircraft wings or helicopter blades. Although some wireless sensors have been reported [7 – 8], they usually include an embedded microprocessor and a radio frequency module to be integrated with the transducer which requires battery power to operate, thus unsuitable for long term monitoring due to limited lifetime and also more frequent maintenance and replacement. Other sensing techniques such as optical fiber-based are compact, light weight, remote sensing capable, but expensive. Therefore, wireless passive strain sensors are highly desirable which can address those mentioned problems.

The concept of Radio Frequency (RF) transducer has been introduced recently through a number of works that address many physical parameters such as pressure, temperature, and also strain [9 – 14]. An RF transducer is a structure that can transform a change of a physical parameter into a change in an RF parameter such as resonant frequency shift, radiation pattern, or a Radar Cross Section (RCS) level change that is readily detectable by a remote system. Ideally, such sensors should be the resonant radiators themselves to eliminate the need for an additional antenna that is the major size factor in these devices. Rectangular and circular patch antennas have been utilized to accomplish those objectives [12 – 13] operating based on frequency shifts, however their sensitivity is limited. Another work based on split ring resonators was employed to build a resonant scatterer sensitive to strain [14], however it is highly dependable on the applied surface and also has low sensitivity. In this paper, we introduce a new design that is based on a patch antenna loaded with an open loop that can achieve significantly higher sensitivity than previous RF strain transducers.

II. Design and Principles of Operation

The new strain transducer design is shown in Fig. 1-2. In this design, a rectangular patch is loaded with a stub on its radiating edge. The stub in turn is connected to an open loop whose resonant frequency depends on the open gap capacitance. The resonant frequency of the open loop, which is determined by the length of the loop, is designed to be close to the dominant resonant frequency of the patch along x direction (Fig. 2). As a result, the structure generates a dual frequency response, in which the separation of the two frequencies is strongly influenced by the capacitance located on the open ring. That means the resonant peaks, especially the one responsible by the open loop, are highly sensitive to the capacitance value at the gap. The open loop here is modified from a traditional open loop, which is the key idea introduced in this work for sensitivity improvement.

Strain is measured by the deformation of a material volume along the strain direction. It is denoted as $_L$ = L/L. The length L_o in the stretched direction is deformed into L as shown in Eq. 1. Strain is unit less and usually measured in % or microstrain (μ) which is 10^{-3} of L/L.

$$L = (1 + \varepsilon_L) L_0 \qquad (1)$$

Therefore, any resonant or antenna structure attempting to transform this change directly into a detectable RF signal is inherently limited as observed in the existing designs [12 – 14]. To solve this problem, we utilize a cantilever

978-1-61284-757-3/11/$26.00 C2011 IEEE

implemented on the open loop that is loaded on a patch antenna instead of using the patch itself alone as in [12].

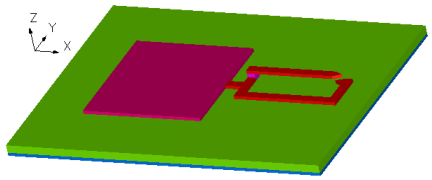

Fig. 1. 3D view of the new Strain sensor design.

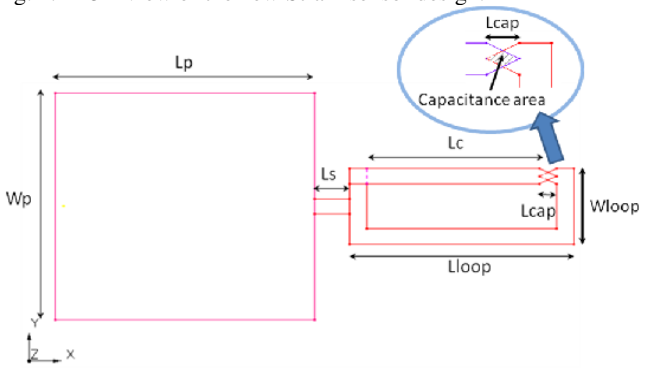

Fig. 2. Top view of the new design of Strain sensor design and zoom in view of the capacitance gap on the open ring.

This cantilever is shorted and fixed at one end of the open loop, while the free end of the cantilever forms a parallel plate capacitor with the other end of the open loop. Thus, the split gap between the two ends of the traditional open ring (Fig. 3a) is transformed into the separation gap of a parallel plate capacitor (Fig. 4).

(a) Traditional open loop (b) Modified open loop

Fig. 3. Top view of traditional and modified loop.

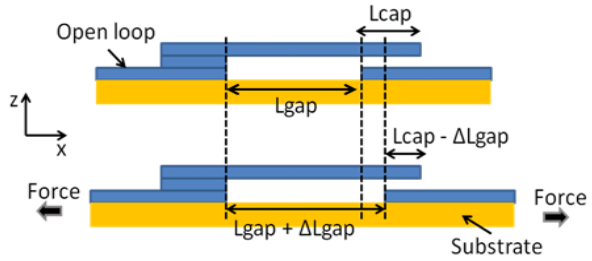

Fig. 4. Cross section view of the cantilever implemented on the modified loop loaded in the new strain sensor.

Therefore, as a certain k% strain is induced on the substrate along x direction (Fig. 4), Lgap is increased by ΔLgap = k% Lgap. Because the cantilever is fixed to the surface only at one end, it is made free from this strain, thus its length, Lc, is constant. Therefore the entire length deformation, ΔLgap is transferred to the change in Lcap (Fig. 4). Effectively, the capacitance is modified by (k% Lgap) instead of (k% Lcap), where Lgap can be engineered to be significantly larger than Lcap as shown in Fig. 2. The use of triangular tips at the loop gap is to further increase the rate of change of the capacitance with a given rate of change of Lcap.

III. Simulations

The transducer is designed to operate around 3GHz, on Kapton substrate 100um thick with dielectric constant of 3.4. In order to model the effects of 1% strain in RF simulations, an increase of 1% in length is applied to each length along the elongation (direction of applied force). These parameters include Lp, Ls, and Lloop. As Lc is fixed and Lloop is increased by 1%, consequently Lcap is decreased by 1% of Lloop. Additionally, the substrate under strain also experiences the Poisson's effect, which essentially causes a contraction in the direction transverse to the strain, thus dimension Wpatch is effectively decreased. Poisson's effect is the ratio of this contraction to the extensions caused by strain. The Poisson's effect can be calculated as shown in Eq. 2, in which w denotes the width of dimension that is transverse to the strain direction, $_p$ is the Poisson's ratio of the Kapton, $_L$ is the applied strain. Other parameters including the Poisson's effect on the substrate thickness and the width of the open loop are negligible to the RF response of the structure, thus are not accounted for. In addition, the resonant frequency of the open loop is found to be little influenced within a few percents of its width, Wloop. Different models with different Lc values, are simulated. Note that, while other values are the same in the model for each Lc, including non-strain and under strain conditions, different Lc values effectively yield different Lcap values as illustrated in Fig. 5. S11 simulations results are presented in Fig. 6 for each Lc values of 500 um, 750 um, and 10000 um, with each Lc value, both strain free and 1% strain conditions are simulated using parameters given in Table I. Notice here the gap between the two parallel surfaces, the lower face of the cantilever free end and the upper face of the open loop end, is set to 10um. This parameter is highly critical for the sensitivity of the strain transducer because it determines the initial gap capacitance.

It is observed from |S11| results in Fig. 6 that each model has a dual frequency response with two close resonant frequencies. The sensitivity of the transducer depends on the value of Lc, which determines the initial capacitance and rate of change of the capacitance as Lcap is decreased. Here, the highest sensitivity that can be achieved is found to be Lc of 9750 um, which induces a frequency shift of 125 MHz at 2.72 GHz, or 4.6% frequency shift per 1% strain. This sensitivity is more than 4 times the sensitivity achieved by rectangular and circular patch antennas previously proposed [12 – 13], which rely only on the change in dimensions of the patches and achieved a sensitivity of only 0.9 – 1.0% frequency shift per 1% strain. It is observed that as the strain is applied, the resonant frequencies are increased which indicates that the capacitance is decreased, thus validating the principle illustrated in Sect. II. Such responses are consistent in all three simulated models (Fig.6).

$$w = (1 - \upsilon_p \varepsilon_L) w_0 \tag{2}$$

978-1-61284-757-3/11/$26.00 C2011 IEEE

TABLE I
Summary of Simulation Parameters

Dimensions (um)	No strain	Strain 1%
Lpatch (Fig. 2)	26000	26260
Wpatch (Fig. 2)	25000	24925
Ls (Fig. 2)	2000	2020
Lloop (Fig. 2)	13000	13130
Wloop (Fig. 2)	5000	5000
c (width of stub and loop)	1000	1000
hsub (substrate thickness)	100	100
hcap (gap between the cantilever and loop)	10	10

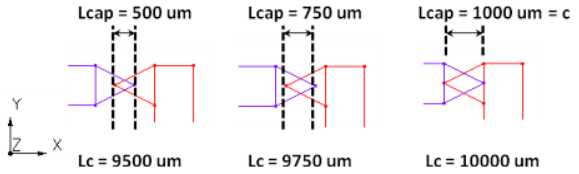

Fig. 5. Different configurations of the tip capacitance as different Lc values, the length of the cantilever, are implemented.

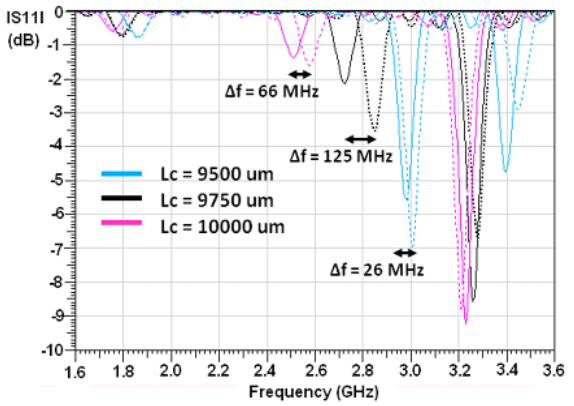

Fig. 6. Different configurations of the tip capacitance as different Lc values are implemented. The solid lines represent non-strain conditions, and the slash lines represent 1% strain conditions.

IV. Prototypes and Measurements

To obtain a rapid fabrication of the transducer in order to validate the newly introduced principle of operation, a prototype of the RF strain transducer as designed in Sect. III is fabricated with a commercial rapid prototyping company. The first portion of the circuit was fabricated on Kapton 100um thick without the cantilever (Fig. 7a). The cantilever is fabricated on a separate substrate of Kapton 50um thick (Fig. 7b). Then the cantilever is manually assembled onto the large circuit in LAAS. In the first portion of the circuit (Fig. 7a), the surface at the tip is cleaned and applied a small amount of transparent adhesive glue spread as thin as possible to create a 10-15um insulating layer, however not well controlled. As this glue layer is dry, the cantilever on Kapton 50um is soldered to the other end of the open loop (Fig. 8) with the copper layer faced down. Then to ensure the cantilever tip copper face is in contact with the glue layer in normal direction but freely to move in elongation direction, a buffer Kapton 127 um is placed on top of the cantilever and pressed down by Scotch tape. In this configuration, as the open loop is stretched, the cantilever can still move freely as the solder end of the cantilever pulls on it. This assembling configuration is illustrated in Fig. 8.

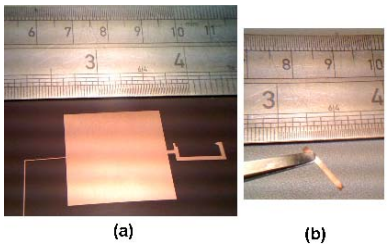

Fig. 7 Two different fabricated portions of the prototype.

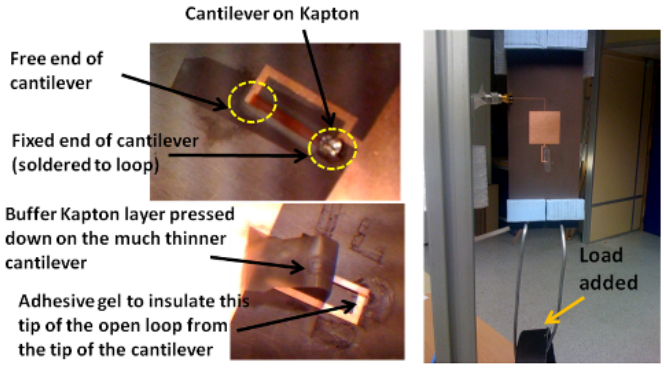

Fig 8. The assembled prototype and measurement setup.

The measurement set up is shown in Fig. 8 in which the strain is increased as the load is added. Measurements of the strain transducer are shown in Figs. 9 -11. Notice that the load is added with irregular intervals due to limited availability of load. Because of such manual process, it is difficult to accurately control the initial gap capacitance of the circuit since the actually Lcap can be easily varied between 750 - 1000 um (Fig. 5). Therefore, it is difficult to tune the circuit's response to the highest sensitivity operation point (Fig. 6). The resulting strain resulted from such setup can be estimated according to Eq. 3 [12], where P is the load, E is the Young's modulus of Kapton, t is the thickness of Kapton, and W is the total width of the Kapton substrate which is 150 mm.

$$\varepsilon_L = \frac{P}{E \cdot t \cdot W} \cdot 100\,\% \qquad (3)$$

Observed in Fig. 9, the two resonant frequencies recorded without any load are 2.9 GHz and 3.4 GHz, which is an excellent agreement with the simulation results (see blue curve in Fig. 6 corresponding to Lc = 9500um). In Fig. 11, a shift of 24 MHz is observed, from 2.914 GHz with no load to 2.938 GHz with 22.5 kg of load, corresponding to 0.645% strain. Equivalently, it is 1.26% frequency shift per 1% strain. The plot of percentage of frequency shift versus percentage of applied strain is shown in Fig. 11 which indicates an excellent linear response for this strain transducer prototype within this

978-1-61284-757-3/11/$26.00 C2011 IEEE

range of strain. Although the prototype is not operating at the most sensitive frequency point as indicated by the black curve in Fig 6., these measurements have successfully validated the novel design and the new principle introduced in this work.

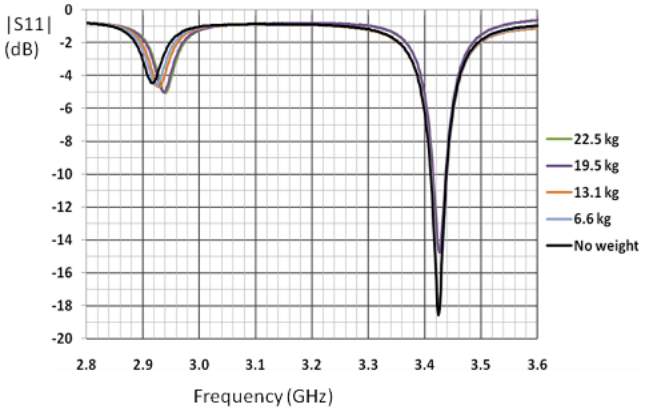

Fig. 9. Measurements of |S11| of the fabricated prototype subjected to different weights attached.

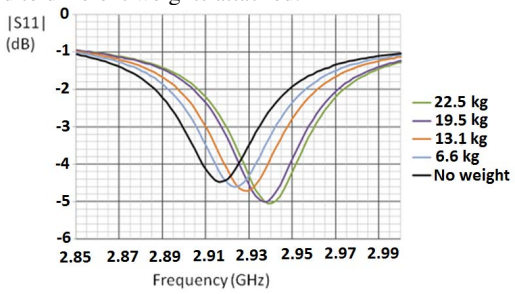

Fig. 10. Measurements of |S11| around 2.9 GHz of the fabricated prototype subjected to different weights.

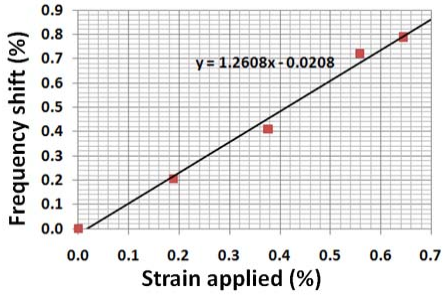

Fig. 11. Plot of % frequency shift versus % strain applied.

IV. Conclusions

A highly sensitive wireless and passive RF strain sensor design is introduced with a novel principle of operation which is successfully validated through experiments. This new idea also enables a new dimension of engineered sensitivity in this type of strain sensing which previously was limited to the linear scale of the changes in the dimensions of the structures. The sensitivity of the proposed design is independent from the material of the applied surface. As an example for a specific passive implementation, the sensor can be interrogated by a radar to monitor its RCS level change as an indicator of strain. In the current design operating at 2.7 – 3 GHz, the sensor can achieve a sensitivity of more than 4 times higher than the existing sensors in the same class. However, in experiments, the currently available prototype achieved a sensitivity of 1.26% frequency shift per 1% strain. Due to limited fabrication capability and rapid assembling, the prototype cannot be built to function at the best operating frequency point, therefore the sensitivity achieved in the current prototype is limited. However, with the well advanced MEMS technology and the simplicity of the design, low cost manufacturing approach of this design can be readily obtained, which is the next step of this work. The sensor can also be easily scaled to operate at millimeter-wave frequencies for higher resolution of strain sensing, or adapted to biomedical applications at lower frequencies.

Acknowledgement

The authors are thankful to the generous help of Tonio Idda in measurements, and to additional assistance of Xavier Dollat and Sofiene Bouaziz in fabrication. The authors would like to acknowledge the support of LAAS-CNRS where this work was performed as well as the support of Georgia Tech.

References

[1] P. C. Chang, A. Flataus, S. C. Liu, “Review paper: health monitoring of civil infrastructure,” Str. Health Mon., vol. 2(3), 2003, pp. 257-267.

[2] B. Rao, The need for condition monitoring and maintenance management in industries Handbook of Condition Monitoring (Amsterdam: Elsevier) pp 1-36, 1996.

[3] R. Melik, E. Unal, N. K. Perkgoz, et. al, “Metameterial-based wireless strain sensors,” Appl. Phys. Lett. 95, 011106 (2009).

[4] W. Staszewski, “Monitoring on-line integrated technologies for operational reliability–Monitor,” Air Sp. Eur., vol.2(4), 2000, pp.67 -72.

[5] K. Sun, Design and characterization of passive wireless strain sensor Master Thesis University of Puerto Rico, 2006.

[6] B. F. Spencer Jr, M. E. Ruiz-Sandoval, N. Kurata, “Smart sensing technology: opportunities and challenges,” Str. Control Health Mon., vol. 5(1), 2006, pp. 29-43.

[7] D. Farhey, “Integrated virtual instrumentation and wireless monitoring for infrastructure diagnostics,”Str. Health Mon.,vol.5(1),2006,pp.29-43.

[8] R. Chacon, F. Guzman, E. Mirambell, et. al, “Wireless sensor networks for strain monitoring during steel bridges launching,” Str. Health Monitoring, vol. 8(3), 2009, pp. 195-205.

[9] J. Chuang, D. Thomson, and G. E. Bridges,“Embeddable wireless strain sensor based on resonant RF cavities,” Rev. Sci. Inst., vol. 76(9), 2005.

[10] M. Jatlaoui, P. Pons, H. Aubert,“Pressure Micro-snesor based on Radio Frequency Transducer,” IEEE/MTT-S IMS, pp.1203-1206, June 2008.

[11] T. Thai, F. Chebila, M. Jatlaoui, et. al. “Design and development of a millimeter-wave novel passive ultrasensitive temperature transducer for remote sensing and identification,” EuMC, pp. 45-48, Sept. 2010, Paris.

[12] U. Tara, H. Huang, R. Carter, et. al., “Exploiting a patch antenna for strain measurements,” Meaurement Sci. Tech., vol. 20(1), 2009.

[13] A. Daliri, A. Galehdar, S. John, et. al, “Circular Microstrip Patch Antenna Strain Sensor for Wireless Structural Health Monitoring,” Proc. World Cong. Eng., vol. 2, London, UK, 2010.

[14] R. Melik, E. Unal, N. K. Perkgoz, et. al, “Metamaterial-based wireless strain sensors,” Appl. Phys. Lett., vol. 95(1), 2009.